PHYSICAL REVIEW B **92**, 235306 (2015)

Atomic clouds as spectrally selective and tunable delay lines for single photons from quantum dots

Johannes S. Wildmann,[1,*] Rinaldo Trotta,[1,†] Javier Martín-Sánchez,[1] Eugenio Zallo,[2,‡] Mark O'Steen,[3] Oliver G. Schmidt,[2] and Armando Rastelli[1]

[1]*Institute of Semiconductor and Solid State Physics, Johannes Kepler University, Altenbergerstraße 69, A-4040 Linz, Austria*

[2]*Institute for Integrative Nanosciences, IFW Dresden, Helmholtzstraße 20, D-01069 Dresden, Germany*

[3]*Veeco Instruments, 4875 Constellation Drive, 55127 St. Paul, Minnesota, USA*

(Received 20 July 2015; revised manuscript received 28 October 2015; published 21 December 2015)

We demonstrate a compact, spectrally selective, and tunable delay line for single photons emitted by quantum dots. This is achieved by fine-tuning the wavelength of the optical transitions of such "artificial atoms" into a spectral window in which a cloud of natural atoms behaves as a slow-light medium. By employing the ground-state fine-structure-split exciton confined in an InGaAs/GaAs quantum dot as a source of single photons at different frequencies and the hyperfine-structure-split D_1 transition of Cs-vapors as a tunable delay medium, we achieve a differential delay of up 2.4 ns on a 7.5-cm-long path for photons that are only 60 μeV (14.5 GHz) apart. To quantitatively explain the experimental data, we develop a theoretical model that accounts for both the inhomogeneous broadening of the quantum-dot emission lines and the Doppler broadening of the atomic lines. The concept we proposed here may be used to implement time-reordering operations aimed at erasing the "which-path" information that deteriorates entangled-photon emission from excitons with finite fine-structure splitting.

DOI: 10.1103/PhysRevB.92.235306 PACS number(s): 78.67.Hc, 78.55.Cr, 78.47.D−, 42.25.Bs

Optically active epitaxial quantum dots (QDs) have emerged as efficient sources of single [1] and entangled photons [2,3] on demand [4] with potential applications in the field of quantum communication [5]. By interfacing photons emitted by QDs with clouds of natural atoms, photon storage at the single-photon level [6] may become possible, thus opening the route to the realization of hybrid interconnects for quantum networking [7]. Pioneering experiments in this field [8] have shown slow light in Rb clouds using single photons emitted by GaAs QDs. These experiments—based on the original concept proposed by Camacho *et al.* [9,10]—were performed by tuning the QD emission lines between the hyperfine-split D_2 transition of ^{87}Rb. Despite that this paper clearly shows the potential of the hybrid natural-artificial atomic interface, the pronounced spectral broadening of the QD-photon source employed for the experiments prevented a detailed analysis of the temporal delay as a function of the relative spectral position of QD and atomic transitions. This is an interesting aspect of the hybrid interface because it could allow introducing temporal delays between photons whose frequencies differ only by a few gigahertz. The resulting spectrally selective delay line could be exploited not only as a filter in experiments aiming at storing and retrieving single photons [6], but it could represent a useful tool to "reorder" in time the temporal sequence of photons originating from radiative cascades in real [11] and artificial atoms [12,13].

In this paper, we demonstrate that a cloud of cesium atoms can be used to introduce a significant temporal delay (up to 2.4 ns for transitions featuring lifetimes $\tau_{QD} \approx 1$ ns) between photons which are separated in frequency by more than 10 GHz. As a source of single photons with different colors, we use the fine-structure-split emission lines of excitons confined in single self-assembled InGaAs/GaAs QDs. Their energy can be finely adjusted to the middle of the D_1 transitions of Cs vapors via external electric or strain fields provided by diodelike nanomembranes [14,15] integrated onto piezoelectric actuators [16,17]. We show that the amount of temporal delay [18] between the photons can be tuned by varying the temperature of the Cs cell and that the "antibunched" character of the quantum source is retained after photon propagation through the vapor. Finally, we develop a theoretical model that quantitatively explains all the experimentally observed features of the spectrally selective delay line.

Figure 1(a) illustrates the idea behind the experiment performed in this paper. We use a single QD as a source of photons with different frequency [see the light blue and the red photons in Fig. 1(a)], and we employ variable strain fields (tuned via application of an electric field F_p through a piezoelectric substrate bonded to the semiconductor layer hosting the QD) or the quantum-confined Stark effect (tuned through an electric field F_p across the QD) to tune their emission energy through the hyperfine-split D_1 lines of a Cs cloud contained in a quartz cell. The photon interaction with Cs atoms in the cell (i.e., the time delay) depends eventually on their energy. When the photon energy matches the center of the D_1 lines [see the uppermost scheme of Fig. 1(a)], the photon group velocity can be drastically decreased with respect to the vacuum value. Therefore, the time sequence of photons emitted by QDs with slightly different frequencies can be controlled by simply varying the temperature of the cell, which increases the optical depth of the absorption line and, due to a change in the real part of the refractive index, modifies also the group velocity.

We start out characterizing the properties of the quartz cell containing the Cs cloud. The Cs D_1 transitions are split into the $6\,^2S_{1/2}$ and $6\,^2P_{1/2}$ levels, which are further split due to the

*johannes.wildmann@jku.at

†rinaldo.trotta@jku.at

‡Current Address: Paul-Drude-Institut für Festkörperelektronik, Hausvogteiplatz 5–7, 10117 Berlin, Germany.

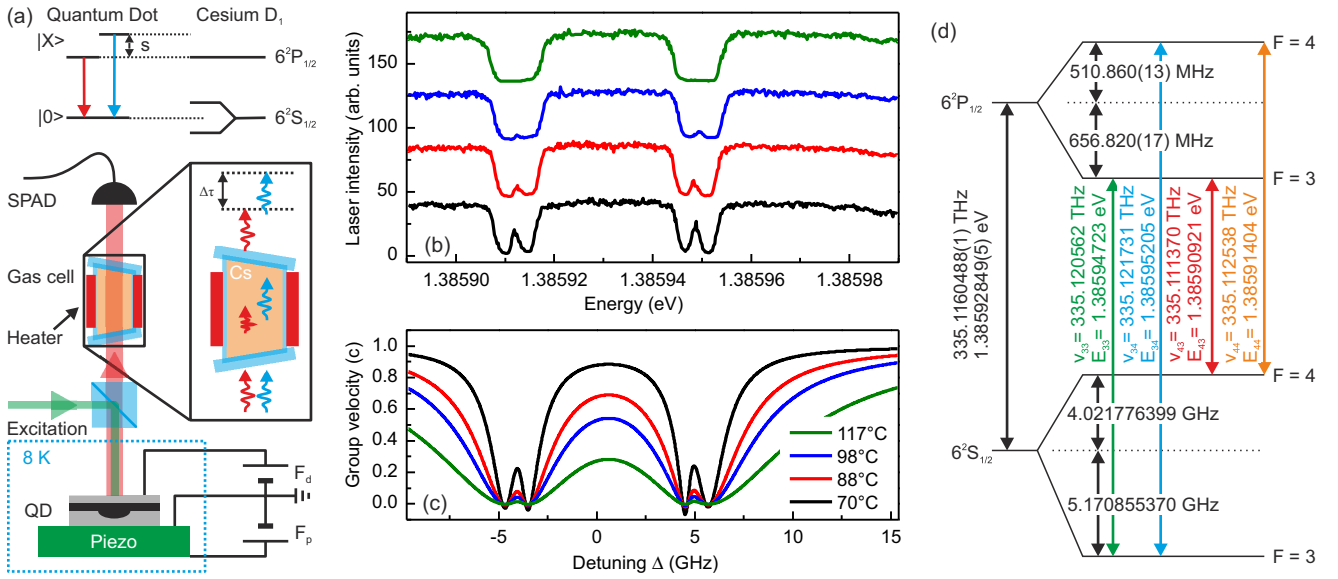

FIG. 1. (Color online) (a) Sketch of InGaAs QD emitting single photons (sketched as wavy arrows) whose energy can be tuned by external stress (F_p) or electric fields (F_d) in the spectral region where a Cs vapor acts as slow-light medium. Among the photons that pass through the atomic vapor, only those which energetically match the spectral region around the hyperfine-split lines of Cs (see the red photons and the energy level scheme on the top) are delayed in time. The arrival time of the photons is detected by a single photon avalanche diode (SPAD) connected to the time-correlation electronics. (b) Transmission spectrum of Cs D_1 absorption lines as a function of the cell temperature. (c) Simulation of group velocity in the proximity of Cs D_1 for different temperatures. (d) Sketch of the allowed transitions of Cs D_1 (indicated by vertical arrows), including hyperfine splitting in the Cs fine structure between the $6\,^2S_{1/2}$ and the $6\,^2P_{1/2}$ levels.

hyperfine coupling into levels characterized by total atomic angular momentum $F = 3$ and $F = 4$. Therefore, there are four possible transitions highlighted in Fig. 1(d) with different colored arrows [19]. The optical transmission measurements around the D_1 lines through the Cs cell are reported in Fig. 1(b) for different vapor temperatures (for details on the measurements see the Supplemental Material [20]). The characteristic four transitions of the hyperfine structure are clearly resolved for a cell temperature $T_{\text{cell}} = 70\,^{\circ}\text{C}$ (black line), but they quickly broaden as T_{cell} is increased due to Doppler broadening [21]. Most importantly, two absorption dips separated by 10 GHz remain for $T_{\text{cell}} > 100\,^{\circ}\text{C}$. This splitting is considerably larger than the one of the D_2 lines of Rb ≈ 6.8 GHz and is therefore more suitable for experiments involving spectrally broadened QD lines (see the following).

Based on these measurements, we are able to simulate the optical response of our Cs cell in the proximity of the D_1 lines. The numerical simulations make use of the susceptibility [9,18] and take into account all possible transitions of the Cs D_1 line. More specifically, the susceptibility of a medium with four resonances (ν_{33}, ν_{34}, ν_{43}, and ν_{44}) can be modeled as

$$\chi(\nu) = A\left(\frac{g_{33}}{\nu_{33}-\nu-i\gamma}+\frac{g_{34}}{\nu_{34}-\nu-i\gamma}+\frac{g_{43}}{\nu_{43}-\nu-i\gamma}+\frac{g_{44}}{\nu_{44}-\nu-i\gamma}\right), \quad (1)$$

where g_{33}, g_{34}, g_{43}, and g_{44} are the oscillator strengths of each resonance, γ is a damping constant determining their linewidth [19], and A is a parameter that increases with the temperature. Finally, the complex refractive index n and the group velocity v_g can be derived from the susceptibility giving

$$v_g(\nu) = \frac{c}{n(\nu)+\frac{dn(\nu)}{d\nu}}. \quad (2)$$

The simulated v_g is shown in Fig. 1(c) for different temperatures as a function of the detuning (Δ) with respect to the Cs D_1 transition. For small Δ, we find that v_g is significantly reduced with respect to the speed of light (c), while there is practically no absorption of the photons propagating through the cell [see Fig. 1(b)]. It is also interesting to note that it is not necessary to tune the energy of the photons exactly in the middle of the hyperfine doublet to observe slow light, as can be clearly seen in Fig. 1(b) for Δ larger than 5 GHz. Finally, we note that the magnitude of the delay can be easily increased by changing the temperature of the cell, revealing that v_g can become negative at the absorption lines. This interesting effect originates from an anomalous dispersion and can either lead to fast light or a backward propagating wave [22].

Having characterized our slow-light medium, we now address the transmission through the Cs cell by streams of photons emitted by semiconductor QDs. We use InGaAs QDs embedded in strain-tunable optoelectronic devices, where large strain and electric fields are used to fine tune the energy of optical transitions across the spectral region of the Cs D_1 line. Details on sample fabrication and device performances can be found elsewhere [23].

Figure 2(a) shows color-coded micro-photoluminescence (micro-PL) spectra of a negatively charged exciton (trion) that

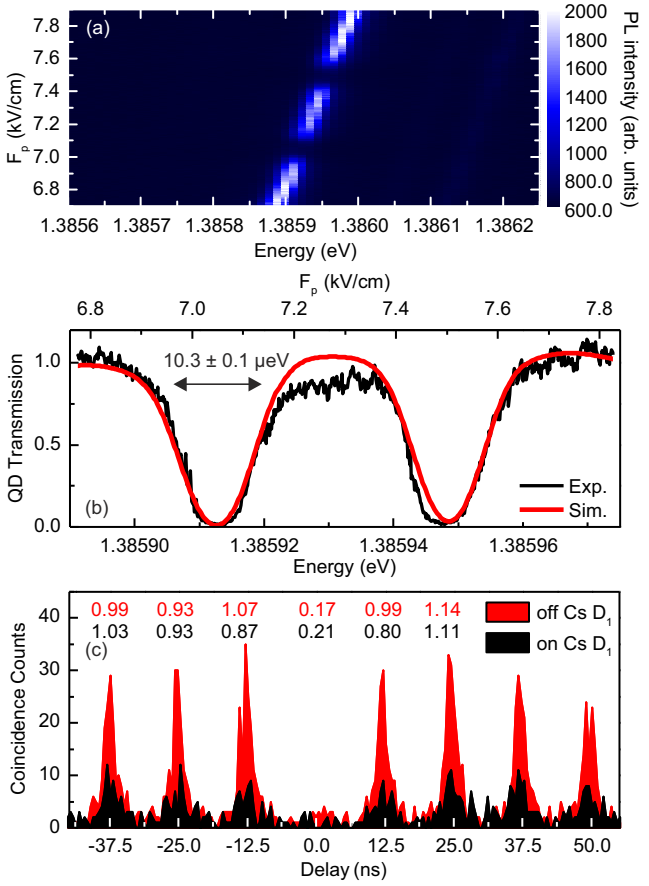

FIG. 2. (Color online) (a) Color-coded micro-PL spectra of a negatively charged exciton (trion) that is scanned through the Cs D_1 by varying the electric field F_p applied to piezoelectric actuator. PL transmission is strongly suppressed at 7.1 and 7.5 kV/cm. (b) Amplitude of the PL as a function of F_p. The solid red line is the result of the theoretical simulation used to extract the linewidth of the trion transition, as explained in the text. (c) Autocorrelation measurements of the trion transition for $\Delta > 15$ GHz (red curve) and $\Delta = 0$ GHz (black curve).

is tuned through the hyperfine structure of Cs D_1 by varying the electric field F_p across the piezo (i.e., the QD strain status, see Refs. [16,17] for more details). A strong quenching of the transmitted light is observed for $F_p = 7.05$ and 7.5 kV/cm as a result of optical absorption in the Cs vapor. This effect can be better observed in Fig. 2(b), where the intensity of the QD light transmitted through the Cs cell is reported as a function of F_p and Δ [a linear relation between the emission energy shift and F_p has been assumed, consistent with the linear shift observed in Fig. 2(a)]. Considering that the temperature of the Cs cell is 136 °C, the data of Fig. 2(b) matches nicely those of Fig. 1(b) but for the additional broadening of the transmission dips. Differently from the case of resonantly excited QDs [24], this effect originates from the broadening of the trion transition under wetting layer excitation. This broadening could not be resolved using our spectrometer (featuring a spectral resolution of 25 μeV), but it instead appears when the QD is scanned through the hyperfine structure of Cs. The experimental data are simulated performing a convolution between the measured Cs transmission spectrum at 136 °C [see Fig. 1(b)] and a Gaussian function. We find the best agreement via least squares minimization and using the linewidth w as the only simulation parameter (see the Supplemental Material [20]). Using this procedure, we extracted $w = 10.3 \pm 0.1$ μeV. On the one hand, this analysis clearly shows that sweeping the QD lines through the hyperfine structure of atomic clouds is a useful tool for high-resolution spectroscopy [25]. On the other hand, the estimated value of w highlights the improved optical quality of our QDs compared to those used in Ref. [26], meaning that the QD line can be conveniently tuned to the middle of the D_1 transitions without substantial photon absorption. This allows us to demonstrate that the antibunching character of the photon source is retained under insertion of a slow-light medium in the optical path. Figure 2(c) shows autocorrelation measurements for photons emitted by a different QD. For these measurements, we used a brighter and short lived trion (although spectrally broader) featuring $\tau_{X^-} = 1.04 \pm 0.1$ ns and $w_{X^-} = 26.1 \pm 0.5$ μeV. The red (black) histogram in Fig. 2(c) shows the result of the experiment for $\Delta > 15$ GHz ($\Delta = 0$). Ideally, the autocorrelation plot for a perfect single-photon source should display a series of peaks of equal amplitude, separated by the inverse of the excitation laser frequency (here 80 MHz) and a missing peak at zero time delay. On the one hand, the measurements for detuning $\Delta >$ 15 GHz show clearly photon antibunching and that the source is a single quantum emitter. On the other hand, it also shows a multiphoton emission probability of $g^{(2)}(0) = 0.17 \pm 0.08$. This latter value most probably arises from carrier recapture phenomena on a timescale comparable with the trion lifetime [27]. The autocorrelation histogram for $\Delta = 0$ shows (i) a very similar multiphoton emission probability of 0.21 ± 0.12, (ii) a reduced number of coincidence counts, and (iii) a broadening of the autocorrelation peaks. While (i) clearly indicates that the antibunched nature of the single-photon source is unaffected by the insertion of Cs vapor in the optical path, (ii) and (iii) can be explained by the broadening of the trion transition (26.1 μeV), which results in higher photon absorption in the Cs vapor and in an enhanced time jitter of photons arrival times [10], as discussed in more details below.

We now demonstrate the possibility of using a Cs cell as a spectrally selective delay line. For these measurements, we use two fine-structure-split emission lines of a neutral exciton from a different QD, and we tune them in energy via the quantum-confined Stark effect resulting from changing the electric field F_d across the p-i-n diode structure (see Ref. [28] for more details). The vertical (V) and horizontal (H) polarized photoluminescence (PL) spectra of the neutral exciton are shown in Fig. 3(a), which reveals a fine-structure splitting of 59 μeV, a value larger than the splitting between the two absorption lines of Cs D_1[41 μeV, see Fig. 1(b)]. The PL intensity for each orthogonally polarized component is shown in Fig. 3(b) as a function of F_d. The two absorption maxima related with the Cs D_1 hyperfine structure can be clearly resolved for both components and, as expected, happen to be at different F_d. This means that, in principle, the temporal sequence of the differently polarized photons escaping from the Cs cell can be varied according to their energetic position with respect to the D_1 transitions of the Cs

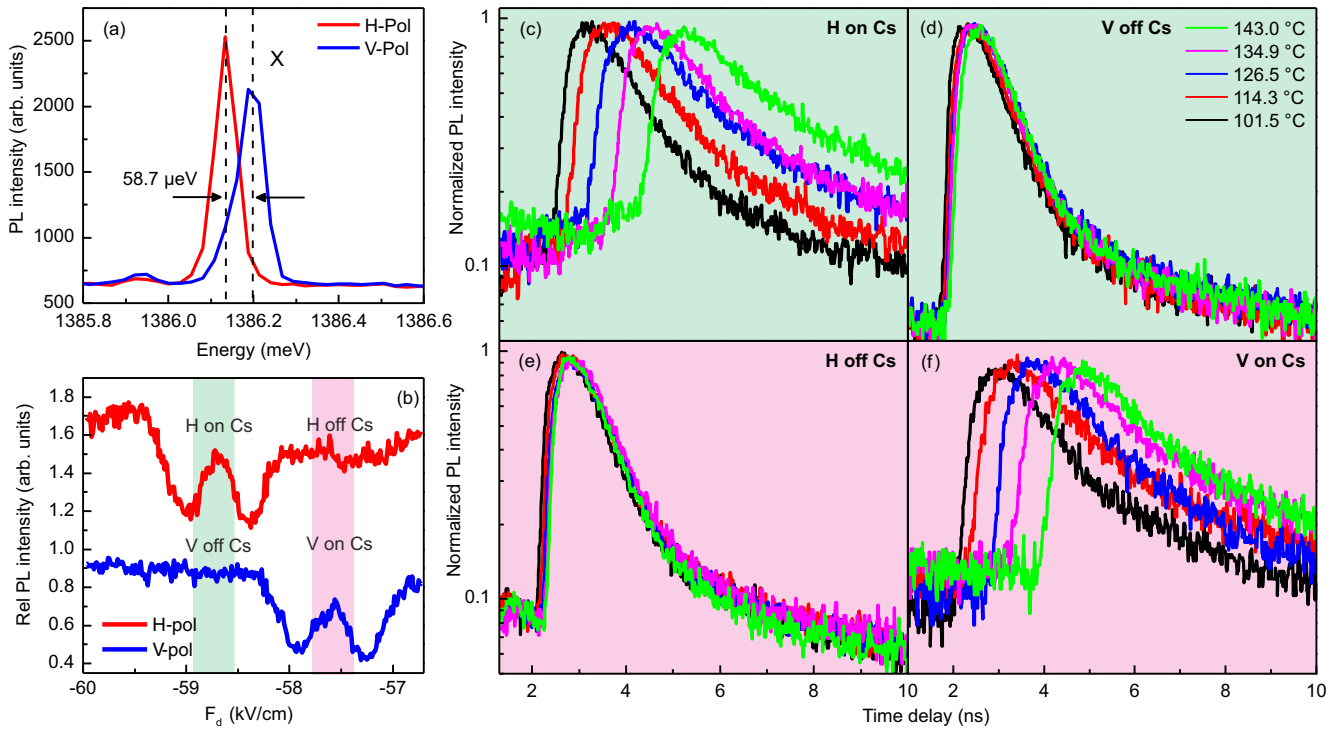

FIG. 3. (Color online) (a) Polarization-resolved PL spectra of the neutral exciton featuring a fine-structure splitting of 59 μeV. (b) Amplitude of both exciton polarization components tuned through the Cs D_1 absorption line via the electric field across the diode F_d. The dips in transmission mark the absorption of the hyperfine structure in Cs. (c)–(f) Time-resolved PL measurements of the fine-structure exciton transition in resonance [(c) and (f)] and out of resonance [(d) and (e)] of the Cs D_1 absorption. The lifetime traces rise at 2 ns due to an offset set in the acquisition electronics.

vapor. Figures 3(c)-3(f) show time-resolved PL measurements at different Cs vapor cell temperatures for $F_d = -58.7$ kV/cm (H-polarized photons tuned to Cs D_1, light green shading) and $F_d = -57.6$ kV/cm (V-polarized photons tuned to Cs D_1, light red shading). There are two main effects: (i) both H- and V-polarized photons can be independently delayed with respect to the detuned case; (ii) the time delay strongly depends on the cell temperature, being larger at higher T_{cell}. More specifically, we measure a shift from 3.2 ns ($T_{\text{cell}} = 101.5\,^{\circ}$C) to 5.1 ns ($T_{\text{cell}} = 143\,^{\circ}$C) in the case of H-polarized tuned photons, and from 2.9 ns ($T_{\text{cell}} = 101.5\,^{\circ}$C) to 4.9 ns ($T_{\text{cell}} = 143\,^{\circ}$C) in the case of V-polarized tuned photons. Negligible time delays were instead measured for all cell temperatures when both, H- and V-polarized photons are detuned by $\Delta = 14.3$ GHz ≈ 59 μeV. Besides the temporal delay, we observe a clear change in the temporal distribution of the transmitted photons, as can be seen by comparing the exponential decays of Figs. 3(c) and 3(d). This finding can be qualitatively explained considering the combined effects of the inhomogeneous broadened QD emission ($w = 6.5$ GHz) and the Doppler broadened absorption of Cs that produce a dispersion of the group velocity and the transmission through the vapor. In order to quantitatively account for the experimental data, we model the QD emission in frequency with a Gaussian distribution featuring the spectral linewidth extracted from Fig. 3(b), while for the time-resolved measurement we use an exponentially modified Gaussian distribution [29] (see Supplemental Material [20]). The temporal distribution of the photon arrival times after propagation through the Cs cell at a specific temperature can be then calculated by discretizing the spectrally broadened QD lines and evaluating (for different detuning Δ) the expected delay and relative intensity. Finally, by integrating over all Δ the time traces as a function of the cell temperature, QD linewidth and detuning can be obtained. Figure 4 shows the result of the simulations for $\Delta = 0$ [Fig. 4(a)] and 59 μeV ($\Delta = 14.3$ GHz) detuning [Fig. 4(b)]. In both cases, we are clearly able to reproduce all the features of the experimental data, thus confirming that the observed temporal distribution of photon arrival times arises from the convolution of the spectrally broadened QD emission with the different group velocities and rate of absorption in Cs vapors. For a better comparison between simulated and experimental results, we extract the values of delays and lifetimes, see Figs. 4(c) and 4(d), respectively. For $\Delta = 0$, the delay of the two excitonic lines (green and blue lines) follows an exponential function with temperature, a trend which is well reproduced by our simulations (see the dashed line). The physical origin of this increase resides on the dependence of the Cs vapor density on cell temperature (see Ref. [19]). This is taken into account in the parameter A of Eq. (1), which is the starting point for calculating the group velocity and, hence, the temporal delay. For large detuning from Cs D_1, a similar exponential increase with temperature is observed. In addition to the shift in delay time, we investigated the broadening of the photon arrival times by considering the changes in the decay time, i.e., the lifetime [see

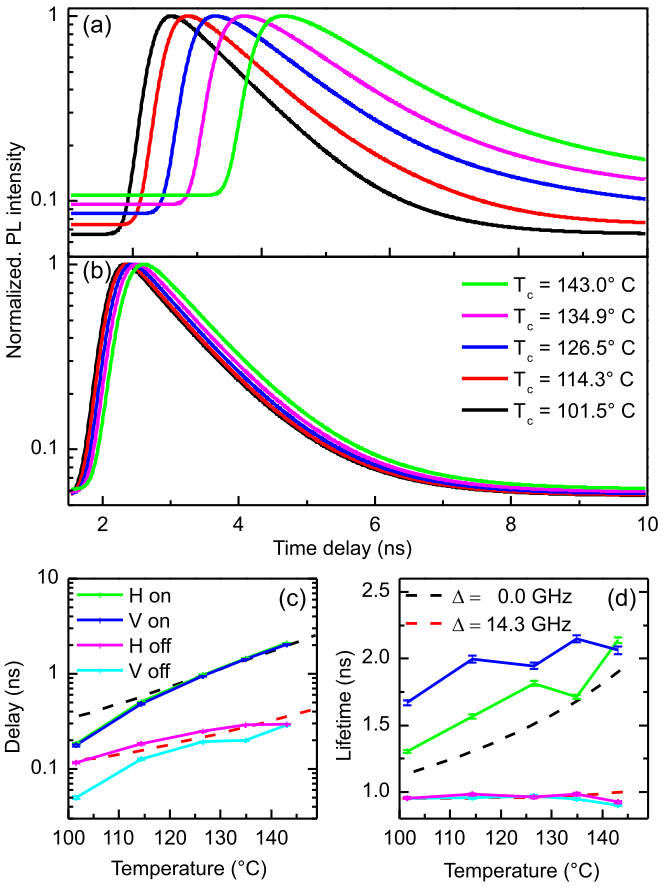

FIG. 4. (Color online) (a) and (b) Numerical simulation of a Gaussian-broadened QD emission line with a detuning of (a) 0 GHz and (b) 14.3 GHz from Cs D_1 at cell temperatures T_{cell} between 101.5 and 143 °C. (c) Temporal delay (offset of 2ns subtracted) as extracted from the simulations (dashed lines) and the experimental data (solid lines) as function of cell temperature. The green, blue, and black curves correspond to $\Delta = 0$ GHz, while the pink, light blue, and red curves show the delay for $\Delta = 14.3$ GHz. (d) Lifetime vs cell temperature as extracted from the experiment (solid lines) and the simulations (dashed lines). Green, blue, and black (pink, light blue, and red) lines correspond to 0 μeV (58 μeV) detuning.

Fig. 4(d)]. The data extracted from the experiments (symbols connected by solid lines) show that for $\Delta = 0$ (blue, green), the lifetime tends to increase with higher cell temperature, while it is almost unaffected for $\Delta = 14.3$ GHz (pink, light blue). Considering the scatter in the experimental data, the observed trends are reproduced fairly well by the simulations (dashed lines).

In summary, we have demonstrated that it is possible to use warm Cs vapors as a spectrally selective and tunable delay line for single photons emitted by semiconductor QD. By performing autocorrelation measurements, we show that the antibunched character of the QD photon source is retained after photon propagation through a slow-light medium made out of an atomic vapor. Then we show that it is possible to introduce a significant temporal delay between photons that are spectrally separated by only a few gigahertz. By tuning the energy of the two fine-structure-split excitons through the hyperfine structure of the D_1 line of Cs via variable strain or electric fields, we were able to slow down independently photons originating from each transition. The measured temporal delay and distribution of the photon arrival times are quantitatively explained by a model that accounts for both the inhomogeneous broadened QD emission and the Doppler broadening of the atomic lines. The spectrally selective delay line we present in this paper can be used to reorder the arrival time of photons emitted during the biexciton-exciton radiative cascade. When used with a QD with suppressed biexciton binding energy [28] and featuring a large fine structure splitting, it may be used to experimentally demonstrate the feasibility of the recently proposed and not yet experimentally demonstrated "time-reordering" scheme for entangled photon generation.

We thank A. Predojević, T. Fromherz, N. Akopian, V. Zwiller, M. Reindl, G. Katsaros, D. Huber, and T. Lettner for the fruitful discussions and F. Binder, A. Halliović, U. Kainz, E. Vorhauer, and S. Bräuer for technical assistance. This paper was supported financially by the EU HANAS (Contract No. 601126) and the FWF (Contract No. I-1190-N20).

[1] J. Kim, O. Benson, H. Kann, and Y. Yamamoto, A single-photon turnstile device, Nature **397**, 500 (1999).

[2] N. Akopian, N. H. Lindner, E. Poem, Y. Berlatzky, J. Avron, D. Gershoni, B. D. Gerardot, and P. M. Petroff, Entangled Photon Pairs from Semiconductor Quantum Dots, Phys. Rev. Lett. **96**, 130501 (2006).

[3] R. M. Stevenson, R. J. Young, P. Atkinson, K. Cooper, D. A. Ritchie, and A. J. Shields, A semiconductor source of triggered entangled photon pairs, Nature **439**, 179 (2006).

[4] M. Müller, S. Bounouar, K. D. Jöns, M. Glässl, and P. Michler, On-demand generation of indistinguishable polarization-entangled photon pairs, Nat. Photonics **8**, 224 (2014).

[5] H. J. Briegel, W. Dür, J. I. Cirac, and P. Zoller, Quantum Repeaters: The Role of Imperfect Local Operations in Quantum Communication, Phys. Rev. Lett. **81**, 5932 (1998).

[6] T. Chanelière, D. N. Matsukevich, S. D. Jenkins, S.-Y. Lan, T. A. B. Kennedy, and A. Kuzmich, Storage and retrieval of single photons transmitted between remote quantum memories, Nature **438**, 833 (2005).

[7] L.-M. Duan, M. D. Lukin, J. I. Cirac, and P. Zoller, Long-distance quantum communication with atomic ensembles and linear optics, Nature **414**, 413 (2001).

[8] N. Akopian, L. Wang, A. Rastelli, O. G. Schmidt, and V. Zwiller, Hybrid semiconductor-atomic interface: slowing down single photons from a quantum dot, Nat. Photonics **5**, 230 (2011).

[9] R. M. Camacho, M. V. Pack, and J. C. Howell, Low-distortion slow light using two absorption resonances, Phys. Rev. A **73**, 063812 (2006).

[10] R. M. Camacho, M. V. Pack, J. C. Howell, A. Schweinsberg, and R. W. Boyd, Wide-Bandwidth, Tunable, Multiple-Pulse-Width

Optical Delays Using Slow Light in Cesium Vapor, Phys. Rev. Lett. **98**, 153601 (2007).

[11] P. Siyushev, G. Stein, J. Wrachtrup, and I. Gerhardt, Molecular photons interfaced with alkali atoms, Nature **509**, 66 (2014).

[12] J. E. Avron, G. Bisker, D. Gershoni, N. H. Lindner, E. A. Meirom, and R. J. Warburton, Entanglement on Demand through Time Reordering, Phys. Rev. Lett. **100**, 120501 (2008).

[13] F. Troiani and C. Tejedor, Entangled photon pairs from a quantum-dot cascade decay: the effect of time reordering, Phys. Rev. B **78**, 155305 (2008).

[14] P. W. Fry, I. E. Itskevich, D. J. Mowbray, M. S. Skolnick, J. J. Finley, J. A. Barker, E. P. O'Reilly, L. R. Wilson, I. A. Larkin, P. A. Maksym, M. Hopkinson, M. Al-Khafaji, J. P. R. David, A. G. Cullis, G. Hill, and J. C. Clark, Inverted Electron-Hole Alignment in InAs-GaAs Self-Assembled Quantum Dots, Phys. Rev. Lett. **84**, 733 (2000).

[15] A. J. Bennett, R. B. Patel, J. Skiba-Szymanska, C. A. Nicol, I. Farrer, D. A. Ritchie, and A. J. Shields, Giant Stark effect in the emission of single semiconductor quantum dots, Appl. Phys. Lett. **97**, 031104 (2010).

[16] S. Seidl, M. Kroner, A. Högele, K. Karrai, R. J. Warburton, A. Badolato, and P. M. Petroff, Effect of uniaxial stress on excitons in a self-assembled quantum dot, Appl. Phys. Lett. **88**, 203113 (2006).

[17] J. D. Plumhof, V. Křápek, F. Ding, K. D. Jöns, R. Hafenbrak, P. Klenovský, A. Herklotz, K. Dörr, P. Michler, A. Schmidt, and O. G. Rastelli, Strain-induced anticrossing of bright exciton levels in single self-assembled GaAs/$Al_xGa_{1-x}As$ and $In_xGa_{1-x}As$/GaAs quantum dots, Phys. Rev. B **83**, 121302(R) (2011).

[18] R. W. Boyd, D. J. Gauthier, A. L. Gaeta, and A. E. Willner, Maximum time delay achievable on propagation through a slow-light medium, Phys. Rev. A **71**, 023801 (2005).

[19] D. A. Steck, Cesium D Line Data. Available online at http://steck.us/alkalidata (revision 2.1.4 December 2010).

[20] See Supplemental Material at http://link.aps.org/supplemental/10.1103/PhysRevB.92.235306 for detailed description of high resolution spectroscopy, numerical simulations, sample fabrication, measurement setup and additional simulation for various linewidth, detuning and Cs cell temperature.

[21] W. Demtröder, *Atoms, Molecules and Photons An Introduction to Atomic-, Molecular- and Quantum-Physics* (Springer Verlag, Berlin, Heidelberg, 2006).

[22] E. Feigenbaum, N. Kaminski, and M. Orenstein, Negative dispersion: A backward wave or fast light? Nanoplasmonic examples, Optics express **17**, 18934 (2009).

[23] R. Trotta, P. Atkinson, J. D. Plumhof, E. Zallo, R. O. Rezaev, S. Kumar, S. Baunack, J. R. Schröter, A. Rastelli, and O. G. Schmidt, Nanomembrane quantum-light-emitting diodes integrated onto piezoelectric actuators, Adv. Mater. **24**, 2668 (2012).

[24] S. M. Ulrich, S. Weiler, M. Oster, M. Jetter, A. Urvoy, R. Löw, and P. Michler, Spectroscopy of the D_1 transition of cesium by dressed-state resonance fluorescence from a single (In,Ga)As/GaAs quantum dot, Phys. Rev. B **90**, 125310 (2014).

[25] N. Akopian, R. Trotta, E. Zallo, S. Kumar, P. Atkinson, A. Rastelli, O. G. Schmidt, and V. Zwiller, An artificial atom locked to natural atoms, arXiv:1302.2005

[26] R. Trotta, J. S. Wildmann, E. Zallo, O. G. Schmidt, and A. Rastelli, Highly entangled photons from hybrid piezoelectric-semiconductor quantum dot devices, Nano Lett. **14**, 3439 (2014).

[27] S. Birindelli, M. Felici, J. S. Wildmann, A. Polimeni, M. Capizzi, A. Gerardino, S. Rubini, F. Martelli, A. Rastelli, and R. Trotta, Single photons on demand from novel site-controlled GaAsN/GaAsN: H quantum dots, Nano Lett. **14**, 1275 (2014).

[28] R. Trotta, E. Zallo, E. Magerl, O. G. Schmidt, and A. Rastelli, Independent control of exciton and biexciton energies in single quantum dots via electroelastic fields, Phys. Rev. B **88**, 155312 (2013).

[29] Y. Kalambet, Y. Kozmin, K. Mikhailova, I. Nagaev, and P. Tikhonov, Reconstruction of chromatographic peaks using the exponentially modified Gaussian function, J. Chemometrics **25**, 352 (2011).